# Design and Fabrication of 3D Fused Quartz Shell Resonators for Broad Range of Frequencies and Increased Decay Time

Mohammad H. Asadian, Yusheng Wang, and Andrei M. Shkel
Microsystems Lab, University of California, Irvine, CA, USA
Email: {asadianm, yushengw, andrei.shkel} @ uci.edu

***Abstract*—This paper presents the design and fabrication of fused quartz 3D shell resonators using high-temperature micro-glassblowing process. We propose novel micro-glassblowing processes allowing to control the operating frequencies without losing the key characteristics of the resonator (symmetry and the Q-factor). A Finite Element (FE) model is presented, demonstrating the self-limiting characteristic of the micro-glassblowing process and predicting the final geometry of the glassblown shells under different process parameters. Three variations of the micro-glassblowing process are presented. A fused quartz shell resonator with n=2 wineglass mode resonant frequency as low as 20 kHz was fabricated using the proposed process, demonstrating a quality factor of 1.7 million. The thermal annealing of the micro-glassblown shells was demonstrated to improve the quality factor of the fabricated shell resonators.**

## I. Introduction

The fabrication processes to realize micro- Hemispherical Resonator Gyroscopes (HRG) can be classified into two main categories: (1) thin-film deposition of the structural materials on pre-etched hemispherical cavities and (2) fabrication based on thermo-plastic deformation. 3D micro shell resonators were fabricated using thin-film deposition of polysilicon [1], silicone dioxide [2], Ultra-Low Expansion (ULE) glass [3], microcrystalline diamond [4], and an Iron-Nickel alloy (Invar) [5]. The thermoplastic deformation processes demonstrated 3D wineglass resonators out of Borosilicate glass [6] , metallic glass [7], [8], and Fused Quartz (FQ) [9]–[11].

The high-temperature micro-glassblowing process was developed to fabricate symmetric wineglass resonators using FQ material [9]. This process consists of (1) isotropic wet etching of annular cavities in an FQ substrate wafer, (2) plasma-assisted wafer bonding of an FQ (or ULE) device wafer to the substrate wafer under atmospheric pressure conditions, and (3) glassblowing in a Rapid Thermal Processing (RTP) furnace at a temperature above the softening point of the FQ (∼1500 °C). At high temperature, the FQ becomes viscous and the cavity pressure increases, forming a 3D symmetric structure. The cavity pressure at the beginning of the process, before shell deforms, is proportional to the glassblowing temperature,

$$P_{ic} = \frac{T_{GB}}{T_{wb}} \times P_{wb}, \tag{1}$$

where $P_{ic}$ is the initial cavity pressure, $T_{GB}$ is the glassblowing temperature, $P_{wb}$ and $T_{wb}$ are the wafer bonding pressure and temperature, respectively. Assuming the glassblowing is an isothermal process, the cavity pressure drops as the enclosed volume increases during glassblowing until an equilibrium with the ambient pressure is reached,

$$P_c = \frac{P_{ic} \times V_{ic}}{V_c}, \tag{2}$$

where $V_{ic}$ is the initial cavity volume, $P_c$ and $V_c$ are the cavity pressure and volume as the shell is deformed. The micro-glassblowing process is a self-limiting process since the continuous pressure drop reduces the deformation rate of the viscous FQ until the equilibrium state, where no further deformation occurs. The equilibrium state depends on the process parameters and defines the final geometry of the glassblown shells.

In this paper, a Finite Element (FE) model is presented to predict the final geometry of the fabricated shells based on the process parameters. For the first time, fabrication of low frequency shell resonators with micro-glassblowing processes are presented and demonstrated experimentally.

## II. Simulation of micro-glassblowing process

The micro-glassblowing process was simulated with a Newtonian isothermal fluid flow model using COMSOL Multiphysics FE package. The temperature-dependent viscosity data

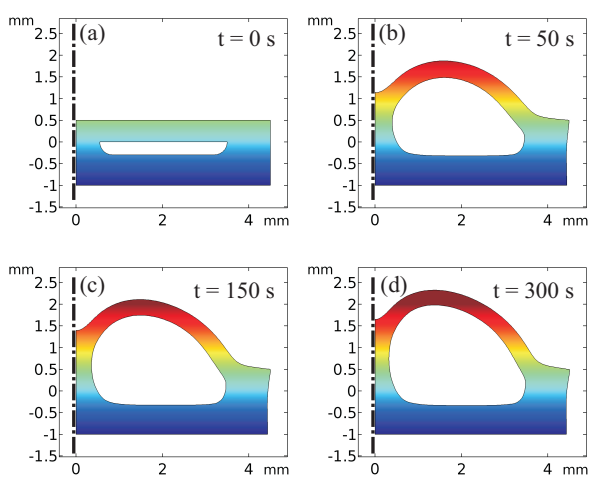


Fig. 1. Time domain representation of the baseline micro-glassblowing process, illustrating simulation results of a 7 mm shell diameter with initial thickness of 500 $\mu$m and stem diameter of 1 mm.

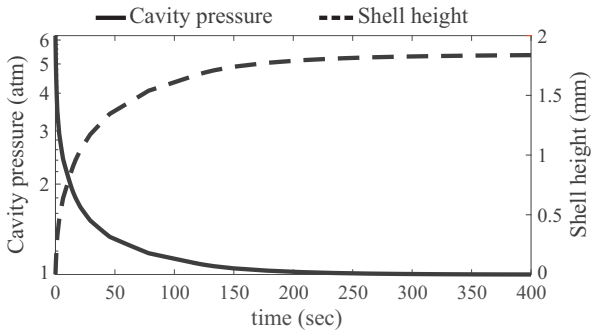


Fig. 2. Illustration of self-limiting characteristic of the micro-glassblowing process; as the pressure (solid line) drops and reaches an equilibrium state with the ambient, the shell deformation rate decreases and limits the shell height (dashed line). Simulations are for a 7 mm diameter shell with 500 $\mu$m thickness.

were obtained from [12]. The viscosity and surface tension of $1.58 \times 10^7$ Pa.s and 0.295 N/m were used for simulation of glassblowing at 1550 °C.

*Baseline micro-glassblowing process*

In the baseline glassblowing process [9], a cavity-etched substrate was bonded to a device wafer at atmospheric pressure and temperature, $P_{wb}$ = 1 atm and $T_{wb}$ = 300 K. This resulted in an initial pressure of $P_{ic} \sim 6.1$ atm at the surface of enclosed cavities. As the shell deforms, the cavity volume increases and pressure drops consequently. The instantaneous volume of the cavity, $V_c$, was calculated using the line integral and centroid of the cavity boundary. The pressure was re-calculated using Eq. 2 at each time step of the simulation. An automatic adaptive re-meshing technique was applied to limit the maximum mesh distortion and to ensure the mesh quality, as the fused silica layer undergoes the large deformations.

Fig. 1 demonstrates the results of a time-dependent FE simulation of the glassblowing process. The cavity pressure and the shell height as a function of simulation time are plotted in Fig. 2. The shell structure deforms until the pressure inside cavity reaches an equilibrium state with the ambient, demonstrating the self-limiting nature of the micro-glassblowing process. The height of fabricated shells depends on the volume of pre-etched cavity, $V_{ic}$, glassblowing temperature $T_{GB}$, wafer bonding pressure $P_{wb}$ and temperature $T_{wb}$, and ambient pressure $P_{ambient}$.

*Vacuum micro-glassblowing process*

The pressure buildup inside the cavities results in a distribution of tensile stresses on the FQ material. The concentration of stress at the edge of the encapsulated cavities may reach the tensile strength of the FQ material, ~50 MPa, resulting the fracture of FQ layer before reaching the softening temperature. A stationary solid mechanics FE model was utilized to compute the maximum tensile stress on an FQ die before glassblowing. The pressure at different temperatures was calculated from Eq. 1 and applied to the cavity surface. The temperature-dependent Young's modulus, Poisson's ratio, and density of FQ were obtained from COMSOL Multiphysics material library. Fig. 3 demonstrates the maximum tensile

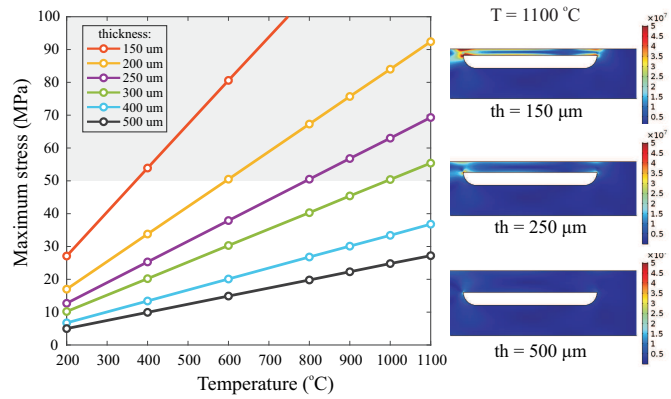


Fig. 3. (left) Simulation results of the maximum tensile stress on FQ dies with different thicknesses as a function of temperature, (right) the stress distribution in solid FQ material with 150, 250, and 500 $\mu$m device layer thicknesses at 1100 °C before the viscous deformation occurs.

stress as a function of temperature for different thicknesses of the device layer. If the tensile stress rises above the strength of solid FQ material, it would cause fracture of the device layer, limiting the minimum thickness of the device layer for the glassblowing process. In our study, the thickness limit of 7 mm diameter shells was 300 $\mu$m.

The wafer bonding at a reduced pressure, $P_{wb} < 1$ atm, decreases the initial cavity pressure, $P_{ic}$, and reduces the maximum stress. Fig. 4 shows the maximum tensile stresses in a 200 $\mu$m thickness device layer bonded at 0.6 and 1 atm pressure. The maximum tensile stress was reduced from 92 MPa to 45 MPa at 1100 °C. The wafer bonding in a partial vacuum reduces the maximum tensile stress and would mitigate the FQ fracture before glassblowing.

Fig. 5 illustrates the height of a shell with 200 $\mu$m thickness bonded under a reduced pressure, $P_{wb} = 0.6$ atm, at different ambient pressures. These results demonstrated that vacuum micro-glassblowing requires wafer bonding and glassblowing in a partial vacuum to fabricate thin FQ shell resonators.

*Reverse micro-glassblowing process*

The vacuum micro-glassblowing process mitigates the stress concentration and fracture of thin device layers at the cost of increased process complexity. The reverse micro-glassblowing process is proposed to reduce internal stresses before the

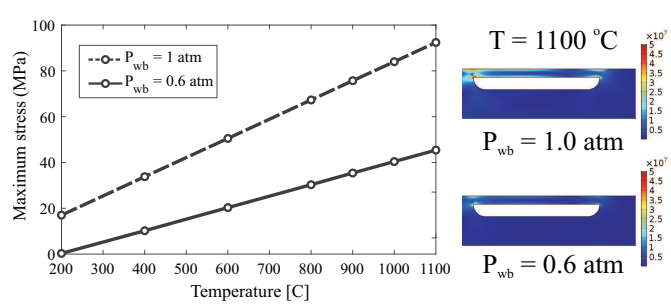


Fig. 4. Wafer bonding at 0.6 atm reduces the maximum tensile stress in a 200 $\mu$m thickness device layer, avoiding the fracture before glassblowing.

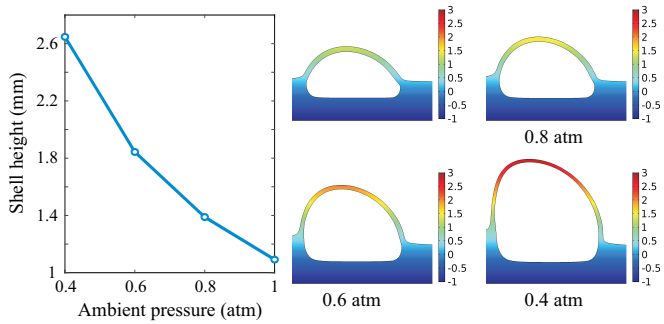


Fig. 5. (left) Glassblowing height of a 200 $\mu$m shell bonded in a partial pressure ($P_{wb}$ = 0.6 atm) under different ambient pressures, (right) final geometry from glassblowing simulations at four different ambient pressures.

viscous deformation regime is reached, demonstrating fabrication of low-frequency shell resonators. In this process, cavities were etched on the device layer. Then, the pre-etched device wafer was bonded to a 1 mm thick FQ substrate wafer. Unlike the baseline micro-glassblowing process, devices were glassblown from the cavity side, reducing the stress concentration due to the round edges formed by an isotropic wet etching, Fig. 6.

Fig. 7 shows fabricated shells with 220 and 150 $\mu$m thicknesses from pre-etching a 500 $\mu$m FQ wafer. The FE simulation results are summarized in Table I.

The glassblown shells were released from the substrate using a parallel back-lapping process. The frequency response of the un-coated released shells was characterized using piezo excitation and Laser Doppler Vibrometer (LDV) detection [13]. Fig. 8 illustrates the Q-factor measurement of the device no. 1 (Table I) using the decay time experiment.

An energy decay time of 17.6 seconds revealed the Q-factor of 1.2 million at 21.8 kHz n=2 wineglass mode (Fig. 8a). After

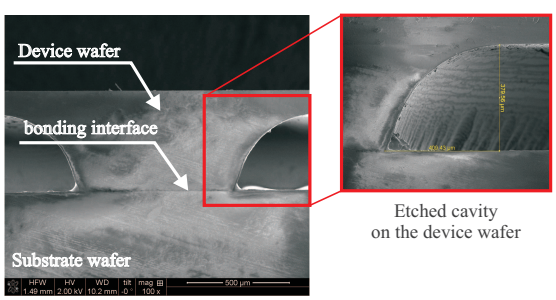


Fig. 6. Etch profile of etched cavity on the device layer showing the round corners around perimeter of the shell.

TABLE I
FE SIMULATION RESULTS FOR THE FABRICATED SHELLS USING REVERSE MICRO-GLASSBLOWING PROCESS

| | Thickness | Etch depth | Simulated shell height | Simulated freq. (n=2) |
|---|---|---|---|---|
| Device #1 | 220 $\mu$m | 280 $\mu$m | 1.70 mm | ~20 kHz |
| Device #2 | 150 $\mu$m | 350 $\mu$m | 2.01 mm | ~16 kHz |

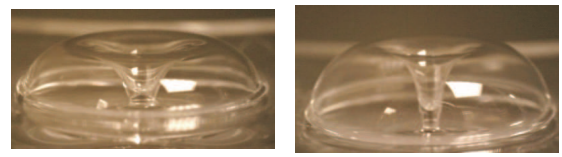


Fig. 7. 7 mm diameter shells with 220 and 150 $\mu$m thickness fabricated in reverse glassblowing process.

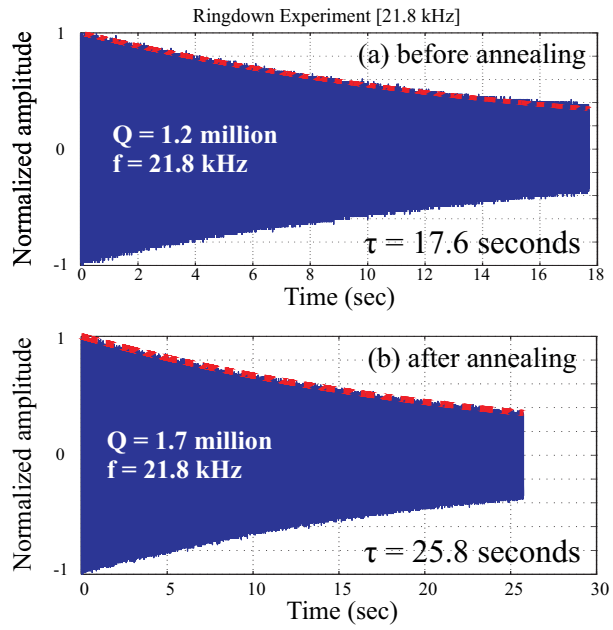


Fig. 8. (a) Decay time constant of a fabricated shell using reverse cavity glassblowing process revealing Q-factor over 1.2 million at 21.8 kHz, (b) thermal annealing improved the Q-factor to 1.7 million.

9 hours thermal annealing at 950 °C with 3 °C/min heating ramp rate, the Q-factor was improved from 1.2 to 1.7 million (Fig. 8b). These preliminary results indicate that thermal annealing improves the Q-factor of glassblown shells [14]. The possible reasons include reduction of residual glassblowing stresses and improvement of the surface quality [15].

## III. Conclusion

An isothermal glassblowing FE model was presented to predict the final geometry of micro-glassblown shells under different process parameters. The limitation of the baseline process in fabrication of low-frequency shell resonators is discussed and two alternative approaches – vacuum micro-glassblowing and reverse micro-glassblowing– were proposed to fabricate low frequency FQ shell resonators without losing symmetry and the quality factor. The Q-factor of 1.2 million was measured on an as-fabricated shell resonator using reverse micro-glassblowing process. Thermal annealing was shown to improve the Q-factor to 1.7 million on the same shell resonator. A lower frequency and a higher Q-factor increase the decay time of FQ resonators, which is a key characteristic for low-power and high-precision navigation and timing applications.

## ACKNOWLEDGMENT

This work was supported by the Defense Advanced Research Projects Agency (DARPA) and U.S. Navy under Contract No. N66001-16-1-4021 at UC Irvine. The design, fabrication, and characterization were performed at the UC Irvine INRF/BiON facility and Microsystems laboratory.

## REFERENCES

[1] P. Shao, C. L. Mayberry, X. Gao, V. Tavassoli, and F. Ayazi, "A polysilicon microhemispherical resonating gyroscope," *Journal of Microelectromechanical Systems*, vol. 23, no. 4, pp. 762–764, 2014.

[2] P. Pai, F. Chowdhury, C. H. Mastrangelo, and M. Tabib-Azar, "Mems-based hemispherical resonator gyroscopes," in *the 2012 IEEE Sensors, Taipei, Taiwan*, October 2012.

[3] Y. Xie, H.-C. Hsieh, P. Pai, H. Kim, M. Tabib-Azar, and C. H. Mastrangelo, "Precision curved micro hemispherical resonator shells fabricated by poached-egg micro-molding," in *the 2012 IEEE Sensors, Taipei, Taiwan*, October 2012.

[4] D. Saito, C. Yang, A. Heidari, H. Najar, L. Lin, and D. A. Horsley, "Microcrystalline diamond cylindrical resonators with quality-factor up to 0.5 million," *Applied Physics Letters*, vol. 108, no. 5, p. 051904, 2016.

[5] N. Mehanathan, V. Tavassoli, P. Shao, L. Sorenson, and F. Ayazi, "Invar-36 micro hemispherical shell resonators," in *the IEEE International Conference on Micro Electro Mechanical Systems (MEMS), San Francisco, CA, USA*, Jan. 2014.

[6] D. Senkal, M. Ahamed, A. Trusov, and A. Shkel, "Demonstration of sub-1 hz structural symmetry in micro-glassblown wineglass resonators with integrated electrodes," in *the International Conference on Solid-State Sensors, Actuators and Microsystems (TRANSDUCERS EUROSENSORS XXVII),Barcelona, Spain*, June 2013.

[7] B. Sarac, G. Kumar, T. Hodges, S. Ding, A. Desai, and J. Schroers, "Three-dimensional shell fabrication using blow molding of bulk metallic glass," *Journal of Microelectromechanical Systems*, vol. 20, no. 1, pp. 28–36, 2011.

[8] M. Kanik, P. Bordeenithikasem, D. Kim, N. Selden, A. Desai, R. MCloskey, and J. Schroers, "Metallic glass hemispherical shell resonators," *Journal of Microelectromechanical Systems*, vol. 24, no. 1, pp. 19–28, 2015.

[9] D. Senkal, M. J. Ahamed, M. H. A. Ardakani, S. Askari, and A. M. Shkel, "Demonstration of 1 million $q$-factor on microglassblown wineglass resonators with out-of-plane electrostatic transduction," *Journal of Microelectromechanical Systems*, vol. 24, no. 1, pp. 29–37, 2015.

[10] J. Y. Cho, J.-K. Woo, J. Yan, R. L. Peterson, and K. Najafi, "Fused-silica micro birdbath resonator gyroscope," *Journal of Microelectromechanical Systems*, vol. 23, no. 1, pp. 66–77, 2014.

[11] W. Li, Z. Hou, Y. Shi, K. Lu, X. Xi, Y. Wu, X. Wu, and D. Xiao, "Application of micro blow-torching process with whirling platform for enhancing frequency symmetry of micro shell structure," *Journal of Micromechanics and Microengineering*, 2018.

[12] R. H. Doremus, "Viscosity of silica," *Journal of Applied Physics*, vol. 92, no. 12, pp. 7619–7629, 2002.

[13] Y. Wang, M. H. Asadian, and A. M. Shkel, "Compensation of frequency split by directional lapping in fused quartz micro wineglass resonators," *Journal of Micromechanics and Microengineering*, vol. 28, no. 9, p. 095001, 2018.

[14] M. J. Ahamed, D. Senkal, and A. M. Shkel, "Effect of annealing on mechanical quality factor of fused quartz hemispherical resonator," in *the IEEE International Symposium on Inertial Sensors and Systems (INERTIAL), Laguna Beach, CA, USA*, Feb. 2014.

[15] Y. Wang and A. M. Shkel, "Study on surface roughness improvement of fused quartz after thermal and chemical post-processing," in *the IEEE International Symposium on Inertial Sensors and Systems (INERTIAL), Laguna Beach, CA, USA*, Feb. 2016.